HDAC7 inhibits cell proliferation via NudCD1/GGH axis in triple-negative breast cancer

MENGDI ZHU[1,2*], NIANQIU LIU[1-3*], JINNA LIN[1,2], JINGRU WANG[1,2], HONGNA LAI[1] and YUJIE LIU[1,2]

[1]Breast Tumor Center; [2]Guangdong Provincial Key Laboratory of Malignant Tumor Epigenetics and Gene Regulation, Sun Yat-Sen Memorial Hospital, Sun Yat-Sen University, Guangzhou, Guangdong 510120; [3]Department of Breast Surgery, The Third Affiliated Hospital of Kunming Medical University, Yunnan Cancer Center, Kunming, Yunnan 650000, P.R. China

Received August 24, 2022; Accepted November 7, 2022

DOI: 10.3892/ol.2022.13619

Abstract. Triple-negative breast cancer (TNBC) is the most malignant subtype of breast cancer. In the absence of effective molecular markers for TNBC, there is an urgent clinical need for promising therapeutic target for TNBC. Histone deacetylases (HDACs), key regulators for chromatin remodeling and gene expression, have been suggested to play critical roles in cancer development. However, little is known ~the functions and implications of HDACs in TNBC treatment in the future. By analyzing the expression and prognostic significance of HDAC family members in TNBC through TCGA and METABRIC databases, HDAC7 was found to be downregulated in TNBC samples and the survival of patients with lower expression of HDAC7 was shorter. Furthermore, HDAC7 was negatively associated with NudC domain containing 1 (NudCD1) and γ-glutamyl hydrolase (GGH). Loss of NudCD1 or GGH predicted improved overall survival time (OS) of patients with TNBC. *In vitro* experiments showed that silencing of HDAC7 enhanced TNBC cell proliferation, while overexpression HDAC7 inhibited TNBC cell proliferation. The results of functional experiments confirmed that HDAC7 negatively modulated GGH and NudCD1 expression. Furthermore, decrease of NudCD1 or GGH inhibited cell proliferation. Notably, the HDAC7-NudCD1/GGH axis was found to be associated with NK cell infiltration. Overall, the present study revealed a novel role of HDAC7-NudCD1/GGH axis in TNBC, which might provide a promising treatment strategy for patients with TNBC.

Correspondence to: Dr Yujie Liu or Dr Hongna Lai, Breast Tumor Center, Sun Yat-Sen Memorial Hospital, Sun Yat-Sen University, 33 Yingfeng Road, Haizhu, Guangzhou, Guangdong 510120, P.R. China
E-mail: liuyujie554@163.com
E-mail: laihn5@mail.sysu.edu.cn

*Contributed equally

Key words: histone deacetylase 7, NudC domain containing 1, γ-glutamyl hydrolase, triple negative breast cancer

Introduction

Breast cancer is a great threat to the life and health of women. According to the global cancer statistics in 2020, breast cancer (BRCA) has surpassed lung cancer as the most prevalent tumor type worldwide and its mortality ranks fourth among all cancers (1). According to the expression level of estrogen receptor (ER), progesterone receptor (PR) and human epidermal growth factor receptor (HER-2), BRCA can be divided into four main types including Luminal A (ER+/PR+/HER2-), Luminal B (ER+/PR+/HER2+), HER2 enriched (ER-/PR-/HER2+) and triple-negative BRCA (TNBC) (ER-/PR-/HER2-). Among these, TNBC, the most malignant subtype, accounts for ~10-20% of all breast cancers (2,3). In addition to the rapid proliferation rate, high aggressiveness and metastatic propensity, the absence of effective molecular markers also remains a challenge to improve the therapeutic effect of TNBC (4). Chemotherapy has remained the only systematic therapy for TNBC thus far. However, due to the high heterogeneity, patients with TNBC are susceptible to developing drug resistance which may lead to disease progression and even mortality (4,5). Therefore, identifying effective prognosis-related molecules and promising drug targets for TNBC is necessary.

Epigenetics refers to reversible, heritable alterations in gene function that do not involve changes in the DNA sequence, including modifications to DNA (e.g., methylation modifications) and various modifications to histones (e.g., histone acetylation and methylation modifications) (6). In recent years, researchers have discovered that epigenetic dysregulation may lead to abnormal gene expression and eventually promote tumor onset and progression (7,8). Acetylation is one of the major post-transcriptional protein modifications in cells. Histone acetylation is controlled by two classes of antagonizing histone-modifying enzymes including histone deacetylases (HDACs) and histone acetyltransferases (HATs) which play a central role in modulating chromatin remodeling and gene expression (9,10). A total of 18 HDACs identified in humans are divided into four classes according to their structures and functions: Class I (HDAC1/2/3/8), class IIa (HDAC4/5/7/9), class IIb (HDAC6/10), class III (SIRT1-7) and class IV (HDAC11). Among these, class I/II/IV are well identified as promising therapeutic targets in cancers (11). Anti-tumor therapy based on drugs targeting

HDACs has also become effective in hematological malignancies, such as lymphoma and multiple myeloma (12-14). It has been reported that multiple HDACs including HDAC1/2/3/6 are dysregulated in BRCA and participate in BRCA progression, metastasis and invasion (12,15,16). In TNBC, HDAC6 has been determined as a possible target and the knockdown or inhibition of HDAC6 can regulate glycolytic metabolism (17). At the same time, inhibition of HDAC6 can enhance tubulin acetylation and has a interaction with eribulin in TNBC (18). HDAC8 is also considered as a promising target in TNBC through Yin Yang 1 and Forkhead Box A1 (19,20). Moreover, several pre-clinical studies have revealed that pan-HDAC inhibitors or some selective HDAC inhibitors exhibit anti-tumor effects through inhibition of EMT pathway in TNBC (20-23). In addition, the class I HDACs (HDAC1/2/3/10) have been shown to be upregulated in TNBC and associated with proliferation, malignant transformation and poor prognosis (24,25). Pre-clinical studies have also revealed the potential synergetic role of HDAC inhibitors with other drugs in TNBC. Sulaiman *et al* (26) showed that the combination of HDAC inhibitors, tamoxifen and mTORC1 inhibitors can suppress the persistence of cancer stem cells and inhibit tumor growth in TNBC. Ma *et al* (27) found that HDAC inhibitors may re-sensitize TNBC cells to tamoxifen treatment. Torres-Adorno *et al* (28) found that HDAC inhibitors can enhance the therapeutic efficiency of MEK inhibitors in TNBC through MCL1 degradation. Multiple studies have revealed the possible synergetic effect of HDAC inhibitors with other drugs in the chemotherapy, radiation therapy and targeted therapy for TNBC (29-33). Chidamide, an oral selective suppressor of class I HDACs, has been proved to be safe and efficacious for the treatment of HR+ advanced BRCA when combined with the aromatase inhibitor exemestane (34), indicating the importance and potential of epigenetic therapy in BRCA. Nonetheless, treatment of TNBC with single HDAC inhibitors have met with disappointing results. Meanwhile, combinations of targeted therapies with HDAC inhibitors are promising treatment options in BRCA, especially in TNBC (27,28,35). Therefore, substantiating that the role of HDACs in TNBC is conductive to prevent TNBC progression.

Biomarkers of cancers not only can play a prognostic role but also can act as drug targets. Due to the development of large-scale sequencing technology, numerous novel biomarkers have been identified in TNBC (36). However, whether HDACs can be used as prognostic predictors in TNBC and whether HDACs-related pathways can be used to assess the potential efficacy of targeted therapies in cancers based on bioinformatics analysis and large-scale sequencing data have not been investigated. Thus, in view of the vital role of HDACs in BRCA, the prognostic value of class I/II/IV HDACs in TNBC and the possible drug targets for patients with TNBC were explored in the present study, principally the expression of HDACs in patients with TNBC and their possible downstream genes based on The Cancer Genome Atlas (TCGA) and METABRIC databases.

Materials and methods

Data source and processing. The RNA-Seq data of 1,247 samples from the BRCA database (139 normal samples and 123 TNBC tumor samples) and corresponding clinical characteristics were downloaded from TCGA website (https://portal.gdc.cancer.gov/projects/TCGABRCA). Ensemble IDs were converted to official gene symbols and log2 processing of the data was performed. mRNAs and protein-coding genes were screened by the Ensemble human genome browser GRCh38 (GRCh38.p9; ftp.ncbi.nlm.nih.gov/genomes/refseq/vertebrate_mammalian/Homo_sapiens/reference/GCF_000001405.39_GRCh38.p13).

Survival analysis. The overall survival of patients with BRCA in the TCGA database was analyzed and plotted on the Kaplan Meir Plotter (https://kmplot.com/analysis/) and the survival in METABRIC database was analyzed and plotted by using Breast Cancer Gene-Expression Miner v4.8 (http://bcgenex.ico.unicancer.fr/BC-GEM/GEM-Accueil.php?js=1). The best cutoff value was taken for all survival analyses.

Comparing HDACs expression. The expression level of genes in TCGA and METABRIC databases was compared and plotted using Breast Cancer Gene-Expression Miner v4.8 (bcgenex.ico.unicancer.fr/BC-GEM/GEM-Requete.php?mode=8) by searching the 'Target Gene Expression' module of the website. The expression of HDAC7 in pan-cancer was analyzed by TIMER (timer.cistrome.org/).

Differential expression analysis. The limma package (37) in R (38) was used to screen the mRNA expression matrix between Low-HDAC7 expression and High-HDAC7 expression groups, TNBC samples and normal tissue samples. The criteria for differential mRNAs were |log 2(fold change)|>1 and a false discovery rate (FDR) <0.05. The volcano map was executed using the OmicStudio tools at https://www.omicstudio.cn/tool.

Functional enrichment analysis. Gene clustering analysis and KEGG analysis were performed on DAVID Bioinformatics Resources (david.ncifcrf.gov/), which allows enrichment of gene symbols by entering gene name files. Then the enrichment results were plotted as bubble map using the ggplot package version 3.3.6 (ggplot2.tidyverse.org) in R studio.

Correlation analysis. To explore the correlation genes with HDAC7, the Sanger box-Spearman correlation coefficients calculator was used to calculated the correlation confidence of HDAC7-related genes, the criteria of correlation genes were |R|>=0.4 and a P<0.05 (39). Then the result was plotted as heat map using the OmicStudio tools V3.3.6 (omicstudio.cn/tool).

Immune correlation. The correlation of the target genes HDAC7, NUDCD1 and GGH was analyzed and the graph was plotted on the TIMER website (http://timer.cistrome.org/) (40). This website used the partial Spearman's correlation to analyze the correlation of target genes expression with immune infiltration level in diverse cancer types. The 'purity adjustment' was used to reduce the confusing effects of tumor purity.

Cell culture. All cell lines were obtained from ATCC, including the normal breast epithelial cell MCF-10A, the luminal BRCA cell lines MCF-7 and T47D and the TNBC cell lines MDA-MB-231, MDA-MB-468, SUM-149, SUM-159

Table I. Cell lines used in the present study.

Name	ATCC catalog no.	ER status	PR status	HER2 status
MCF-10A	CRL-10317	-	-	-
MCF-7	HTB-22	Positive	Positive	Negative
T47D	HTB-133	Positive	Positive	Negative
MDA-MB-231	HTB-26	Negative	Negative	Negative
MDA-MB-468	HTB-132	Negative	Negative	Negative
SUM-149	TCP-1001	Negative	Negative	Negative
SUM-159	TCP-1002	Negative	Negative	Negative
BT-549	HTB-122	Negative	Negative	Negative

ER, estrogen receptor; PR, progesterone receptor; HER2, human epidermal growth factor receptor.

and BT-549. MCF-7, T47D, MDA-MB-231, MDA-MB-468, SUM-149, SUM-159 and BT-549 cells were cultured in DMEM (Gibco; Thermo Fisher Scientific, Inc.) with 10% fetal bovine serum (FBS, Newzerum Ltd.). MCF-10A cells were cultured in the special medium (HY Bio, Guangzhou, China) supplemented with 5% horse serum, 20 ng/ml EGF, 100 ng/ml cholera toxin, 0.01 mg/ml insulin, 500 ng/ml hydrocortisone (Procell). The detail information of each cell line is in Table I.

Cells were cultured using the medium described above and the medium was changed every 2 days. When the cell density reached ~70-80%, cell passaging was performed. The medium was removed and 1 ml trypsin was added to digest cells for ~30 sec-1 min, then 1 ml medium containing serum was added to terminate digestion. Cells were gently blown off the bottom of the culture bottles, then transferred to a 15 ml centrifuge tube and centrifuged at room temperature, 100 g for 3 min. The liquid was removed and cells were resuspended with 1 ml complete medium. Cells were passage into a new culture bottle at 1:3-1:4. The number of cell passages in a single experiment did not exceed 15 times.

Small interfering (si)RNA transfection. For transfection of siRNA, cells were plated at a density of $1x10^5$ cells per well in 6-well plates, cell density was ~60-80% per well. Then cells were transfected with negative control (NC), or specific siRNAs for HDAC7, NudCD1 and GGH (100 nM; Shanghai GenePharma Co., Ltd.), respectively, using Lipofectamine® RNAiMAX transfection reagent (Invitrogen; Thermo Fisher Scientific, Inc.). For transfection, 125 μl opi-MEM (Thermo Fisher Scientific) was mixed with 25 pmol siRNA and another 125 μl opi-MEM was mixed with 7.5 μl RNAiMAX and the mixture was incubated at room temperature for 15 min respectively. Then the iMAX solution was added to the siRNA solution, mixed well and incubated at room temperature for another 15 min. Finally, the 250 μl mixture was added into indicated wells. After transfection of 24 h, the culture medium was aspirated and replaced with new complete medium for another 24 h.

The siRNA sequences were: HDAC7: 5'-ACUUCUUGG GCUUAUAGCGCA-3', 5'-CGCUAUAAGCCCAAGAAG UCC-3'; NUDCD1: 5'-AGUGUAUAUUGAUCAUCUCGA-3', 5'-GAGAUGAUCAAUAUACACUGG-3'; GGH: 5'-UUU UUGCAUUAAUAUUCCGAU-3', 5'-CGGAAUAUUAAU GCAAAAAUG-3'; NC: 5'-UUCUCCGAACGUGUGACG UTT-3', 5'-ACGUGACACGUUCGGAGAATT-3'.

Construction of plasmid and transfection. pCMV-MCS (catalogue number: JD2022092202R) cloning vector was used to construct pCMV-HDAC7 over-expression plasmid. Plasmid was transfected into cells with Lipofectamine® 3000 (cat. no. L3000150; Invitrogen; Thermo Fisher Scientific, Inc.). Cells were seeded in 6-well plates at $1x10^5$ cells per well and transfection experiments were performed when the cell density reached 60-70%. The transfection system was 1.5 μg of plasmid, 3 μl p3000 and 3 μl Lipofectamine® 3000 per 250 μl of opi-MEM. The transfection mixture was incubated at room temperature for 15 min and added into the six-well plates. After 24 h of transfection, the supernatant was discarded and the medium was changed to complete medium and incubated for another 24 h for subsequent experimental verification.

RNA extraction. Total RNA was extracted from BRCA cells using TRIzol® (Thermo Fisher Scientific, Inc.) and RNA concentration and quality were determined by the absorbance of RNA at 260 and 280 nm. RNA extraction, cDNA synthesis, and qPCR performed according to the manufacturer's protocol. Each six-well plate ($1-2x10^5$ cells per well) was lysed with 1 ml of TRIzol® and then the lysis was transferred to 1.5 ml EP tubes. To let the RNA and protein in cell phase separation, the lysis was mixed with 200 μl of chloroform. The mixture was centrifuged at 4˚C, 12,000 x g for 15 min. The upper layer of clear liquid was carefully transferred to another 1.5 ml EP tube for the next reaction. The clear liquid was gently mixed with 500 μl of isopropyl alcohol and left to stand for 10 min at room temperature. Then the mixture was centrifuged at 4˚C, 12,000 x g for 10 min and the supernatant was discarded, leaving an RNA precipitate. The precipitate was gently washed with 1 ml of 75% ethanol. Then the liquid was centrifuged at 4˚C, 7,500 x g for 5 min and the supernatant was discarded. The precipitate was dried for 10 min and dissolved with 30-50 μl RNA free-DEPC H_2O. Total RNA concentration and purity were analyzed in duplicate using a NanoDrop One (cat. no. AZY1705838; Thermo Fisher Scientific, Inc.). PrimerScript RT Master Mix (cat. no. RR036A; Takara Bio, Inc.) was used to generate cDNA. Then, 2 μl of 5X PrimerScript RT master

mix, 1,000 μg of RNA and DEPC water were used per 10 μl of reverse transcription reaction system.

Reverse transcription-quantitative (RT-q) PCR. The reverse transcription procedure was: 15 min at 37˚C, 5 sec at 85˚C and then 4˚C for 30 min. RT-qPCR was performed using TB Green Premix Ex Tap II (cat. no. RR820A; Takara Bio, Inc.). The RT-qPCR system contained 5 μl SYBR Premix Ex Taq II, 0.4 μl forward primer, 0.4 μl reverse primer, 3.2 μl DEPC water and 1 μl cDNA product. The reactions were carried out in a LightCycler480 (Roche, America) system. The reaction protocol was: 95˚C for 10 min; followed by 40 cycles at 95˚C for 10 sec and 60˚C for 30 sec. The quantification method is as follows: $2^{-\Delta Cq}$ (41). The experiment was repeated independently three times. The gene-specific primer sequences were: GAPDH: 5'-ggAgCgAgATCCCTCCAAAAT-3', 5'-ggCTgTTgTCATACTTCTCATgg-3'; HDAC7: 5'-TgCCCAgTCCTTAATgACCAC-3', 5'-CACCTggACgTgAgTTTTgAg-3'; NudCD1: 5'-AAAACCACgAgAggTgTTTCg-3', 5'-CTgACAAggTAACCCAggTAgA-3'; GGH: 5'-ggAgAgTgCTTATTAACTgCCAC-3', 5'-AggCTCCACTTATggAAATTgg-3'.

Cell viability assays. Following transfection with specific siRNAs, cells were plated at 3,000 cells per well in 96-well plates and cultured for the indicated time periods. Cell viability was performed using the MTT assay (cat. no. 3580MG250, BioFrox). Briefly, MTT was configured into a 5 mg/ml solution in sterile phosphate-buffered saline (PBS) and added into cell culture media with a ratio of 1:10 at 0 (6 h after plating was identified as 0 h; when the cells were attached), 24, 48 and 72 h, respectively. Following incubation at 37˚C for 4 h, the culture medium was aspirated and the precipitate was dissolved in DMSO, then absorbance at a wavelength of 490 nm was detected by a microplate spectrophotometer. The 24, 48 and 72 h absorbance was compared with the day 0 absorbance in each group and the fold change of relative cell viability plotted using GraphPad Prism 8.0 software (GraphPad Software, Inc.).

Colony formation assay. For colony assay, following transfection with siRNA for 48 h, cells were plated at 1,000 cells per well in 6-well plates and cultured with the complete culture medium for 14-21 days. Then the culture medium was removed and cells were fixed with 4% paraformaldehyde at room temperature for 15 min and stained with 0.1% crystal violet for 20 min. The colony formation was imaged and automatic counting using a fluorescent enzyme-linked immune-spot analyzer (AID vSpot Spectrum; Advanced Imaging Devices GmbH). Groups were compared using cell colony counts.

Statistical analysis. All statistical analyses were performed using GraphPad Prism 8.0 (GraphPad Software, Inc.), unless otherwise described in the figure legends or methods. One-way ANOVA with Dunnett's multiple comparisons was used to compare the mRNA expression of HDACs in different subtypes of BRCA in TCGA and METABRIC databases. Two-tailed unpaired Student's t-test was employed to test the significance between two groups. Kaplan-Meier survival curve and Log-rank test were used to analyze the survival outcomes. The univariate Cox regression analysis was used to explore the prognostic value of HDAC7 in TNBC. Pearson's correlation was used to investigate the relationship between HDAC7 and downstream genes and immune cells infiltration. All experiments for cell cultures were performed independently at least three times and standard deviation (SD) was used to measure the variation. $P<0.05$ was considered to indicate a statistically significant difference.

Results

Expression of the histone deacetylases in TNBC. Patients with TNBC were identified as ER negative, PR negative and HER2 negative based on IHC information from the database. The mRNA expression level of HDACs was analyzed in a total of 126 and 289 cases of patients with TNBC from TCGA-BRCA database and METABRIC dataset, respectively. It was observed that HDAC1/2/8/9 were upregulated in the tissue samples of BRCA, especially in TNBC ($P<0.01$), while HDAC3/4/5/6/7/10 were downregulated in BRCA and TNBC tissues ($P<0.01$) in the TCGA database. HDAC11 expression was reduced in TNBC samples but significantly upregulated in non-TNBC samples (Fig. 1A). The P-values in HDAC1-8 and HDAC10-11 indicated the significance between the ER-group and the normal tissue group. The P-value of HDAC9 represented a significant difference between TNBC and non-TNBC groups and no significant difference was noticed in HDAC9 expression between TNBC group and normal group. Since normal tissue samples are unavailable in METABRIC database, the expression of target HDACs in TNBC samples were compared with non-TNBC samples. The results showed that the expression of HDAC1/2/4/6 was higher in TNBC than in patients without TNBC ($P<0.05$). HDAC3/7/11 was significantly lower in TNBC samples ($P<0.01$; Fig. 1B). However, no statistical difference was noticed in HDAC5/8/9 expression levels between TNBC and non-TNBC groups (Fig. S1A). HDAC10 was not detected in the METABRIC database. The expression of HDAC1/2/3/7/11 in TNBC and non-TNBC groups were consistent with the results from the two databases.

Prognostic value of the histone deacetylases for TNBC. To further identify the prognostic value of HDACs in TNBC, the Kaplan-Meier Plotter online website was used to analyze the prognostic value of HDACs in the TCGA database and the Breast Cancer Gene-Expression Miner online website (http://bcgenex.ico.unicancer.fr/BC-GEM/GEM-Accueil.php?js=1). First of all, it was found in TCGA database that only HDAC7 and HDAC9 expression were significantly associated with overall survival time (OS) in patients with TNBC and lower expression of HDAC7 [Hazard ratio (HR)=0.43; 95% confidence interval (CI)=0.19-0.95, P=0.031] and HDAC9 (HR=0.34; 95%CI=0.15-0.75; P=0.0053) were associated with poor survival rate (Fig. 2A). Secondly, in METABRIC database, the results showed that HDAC5/6/7/9 expression was significantly associated with the survival time of patients, of which high expression of HDAC5 (Hazard Ratio HR=1.43; 95%CI=1.03-2.01; P=0.0353) and HDAC6 (HR=1.44; 95%CI=1.00-2.07; P=0.0496) were associated with shorter OS, while high expression of HDAC7 (HR=0.66; 95%CI=0.49-0.88; P=0.0052) and HDAC9 (HR=0.63; 95%CI=0.40-0.99; P=0.0457) were associated with improved OS time (Fig. 2B). The expression of HDAC1-6, HDAC8, HDAC10 and HDAC11 was not statistically correlated

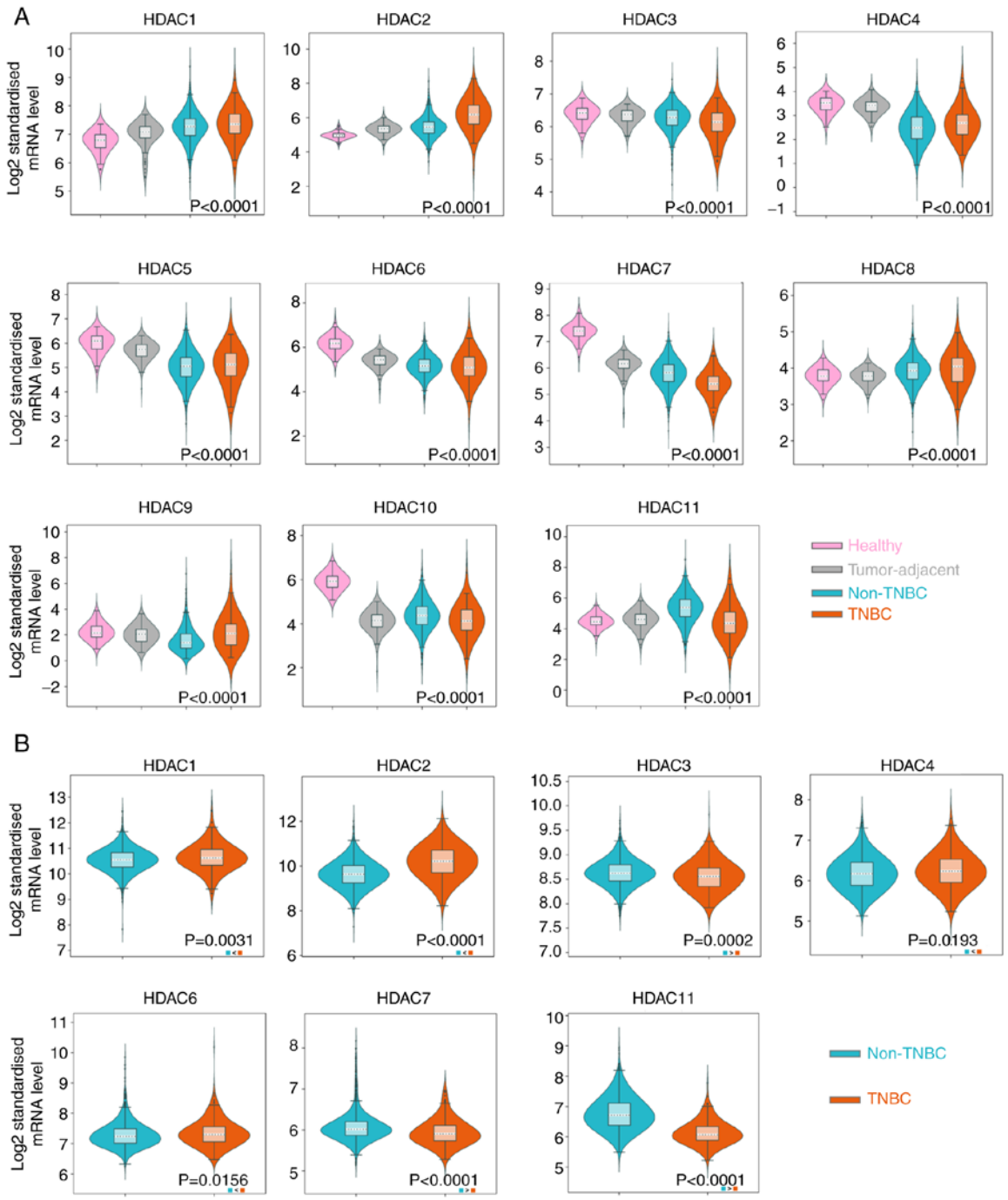

Figure 1. Differentially expressed HDACs in the TCGA and METABRIC databases. (A) expression of HDAC1-11 in the TCGA database. HDAC1/2/8/9 were upregulated in TNBC compared with normal tissue (P<0.05). HDAC3/4/5/6/7/10/11 were downregulated in TNBC compared with normal tissue (P<0.05). (B) Expression of HDACs in the METABRIC database. HDAC1/2/4/6 were upregulated in TNBC compared with non-TNBC (P<0.05). HDAC3/7/11 were down-regulated in TNBC compared with non-TNBC (P<0.05). HDAC10 was not detected. HDACs, histone deacetylases; TCGA, The Cancer Genome Atlas; TNBC, triple-negative breast cancer.

with OS time in the TCGA database (Fig. S1B). Moreover, the expression of HDAC1-4, HDAC8, and HDAC11 was not statistically correlated with OS time in the METABIRC database (Fig. S1C). In summary, the two datasets indicated HDAC7 was downregulated in BRCA, especially in TNBC tissues and lower expression of HDAC7 predicted poor OS time.

As the above analysis suggested that HDAC7 might serve as a tumor suppressor in BRCA, the role of HDAC7 in other cancer types was further evaluated by the TIMER website. The results indicated that HDAC7 was downregulated in a number of cancers including BRCA, kidney chromophobe, lung adenocarcinoma, lung squamous cell carcinoma and uterine corpus endometrial carcinoma, which indicated the possible inhibitory role of HDAC7 in cancers (Fig. 2C). Overall, these results suggested that HDAC7 might be a promising prognostic indicator and therapeutic target for cancers, especially for TNBC.

Functional enrichment analysis of HDAC7 in TNBC. To further assess the predictive value of HDAC7 in TNBC, the Univariate Cox regression analysis was used. The hazard ratio

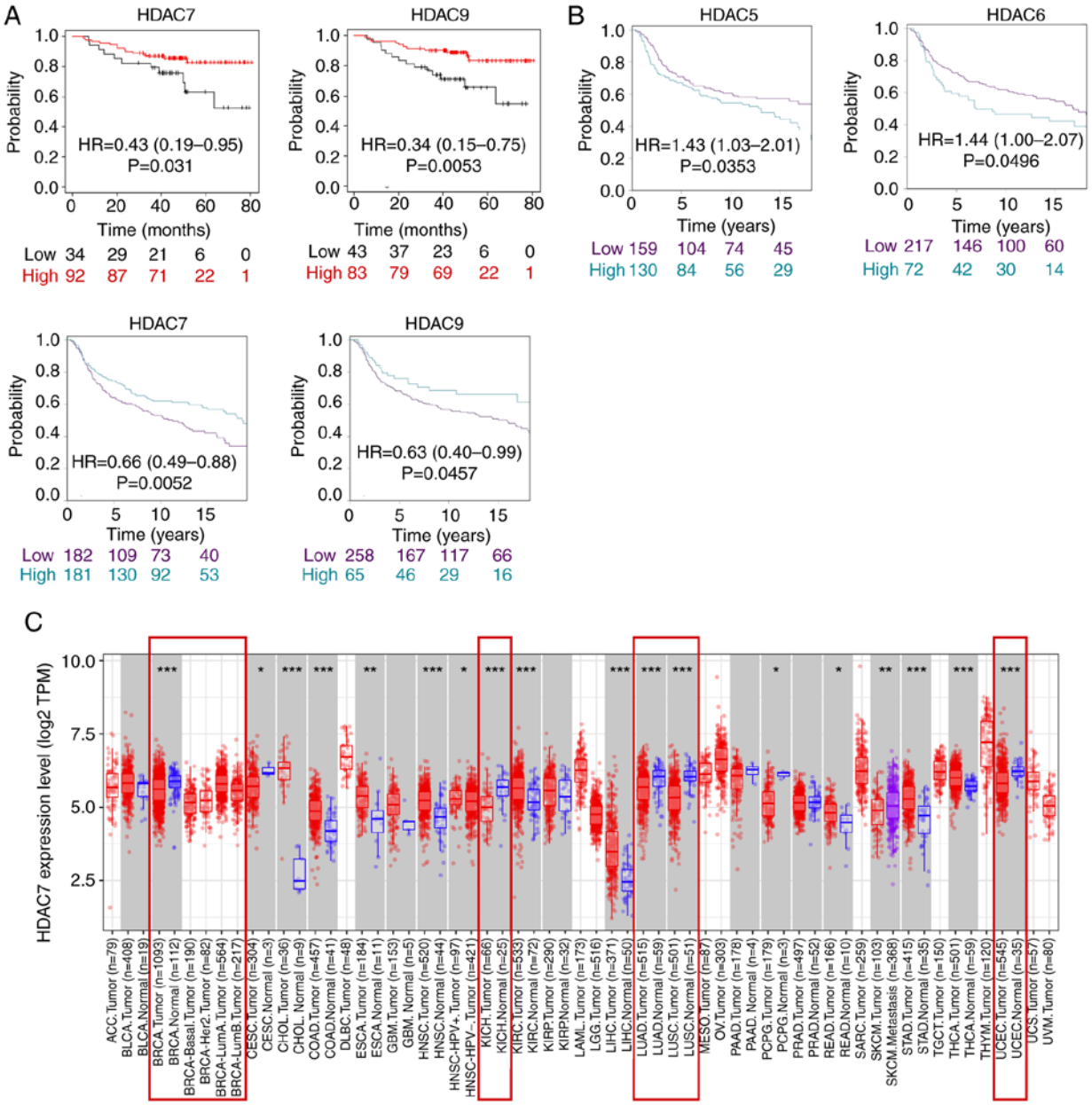

Figure 2. Prognostic value of the histone deacetylases for TNBC. (A) Kaplan-Meier survival analysis showed that HDAC7 and HDAC9 were associated with prognosis in TNBC in the TCGA database (P<0.05). (B) Kaplan-Meier survival analysis showed that HDAC5/6/7/9 were statistics associated with prognosis in TNBC in the METABRIC database (P<0.05). (C) The pan-cancer expression of HDAC7. The red boxes indicate cancers in which HDAC7 expression is downregulated compared with normal tissues. TNBC, triple-negative breast cancer; HDACs, histone deacetylases; TCGA, The Cancer Genome Atlas.

(HR) of HDAC7 in TNBC was 0.389 (95%CI=0.153-0.99), P=0.048 (Fig. 3A), validating that HDAC7 might function as an independent prognostic factor. As shown in Fig. 2A, patients with TNBC in TCGA database were divided into HDAC7 high expression group (n=89) and low expression group (n=34) according to the optimum cutoff value based on the association with OS. Then the expression of differential genes between the two groups were analyzed and KEGG enrichment analysis was performed to explore the biological function of HDAC7 (Fig. 3B and C). The orange and yellow dots in Fig. 3B represented differentially expressed genes that have no statistical significance, or the |log 2 (fold change)|≤1. The blue and red dots in Fig. 3B represented the differentially expressed genes that have statistical significance or whose |log 2 (fold change)|>1. Those significantly upregulated or downregulated genes were used to perform the KEGG enrichment analysis. As shown in Fig. 3C, differentially expressed genes were mostly involved in neuroactive ligand-receptor interaction, cell adhesion molecules, PI3K-Akt signaling pathway and cytokine-cytokine receptor interaction pathway (P<0.05, Fig. 3C), which indicated the possible role of HDAC7 in the regulation of TNBC progression.

NudCD1 and GGH prognostic genes are HDAC7-related downstream genes. As our previous analyses have identified HDAC7 as a predictive gene with significant clinical value and biological functions in TNBC, genes that regulated by HDAC7 and participating in TNBC progression were next explored. Histone deacetylases remove acetyl groups from histone and tighten DNA-histone interactions, resulting in a closed

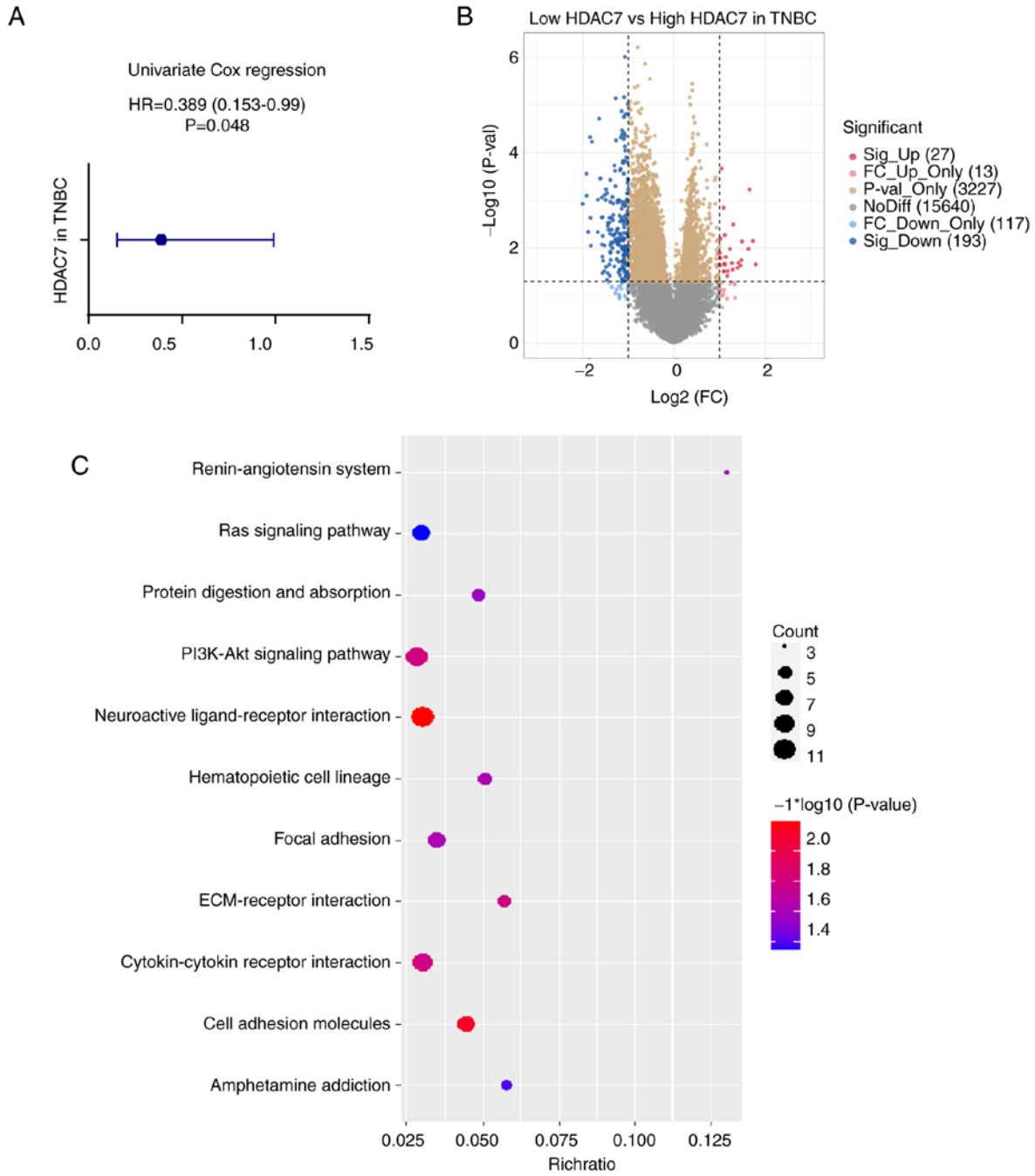

Figure 3. Functional enrichment analysis of HDAC7 in TNBC. (A) Univariate cox regression analyzes of HDAC7 in TNBC. HR=0.389 (0.153-0.99), P=0.048. (B) Volcano plot of differentially expressed genes between the high and low HDAC7 expressing groups in TNBC. (C) Bubble plot of KEGG clustering of differentially expressed genes, the bubble size represents the cluster count, the color represents the P-value and the position of the horizontal axis represents the enrichment ratio. All the analysis data was obtained from the TCGA database. *P<0.05, **P<0.01, ***P<0.005. HDACs, histone deacetylases; TNBC, triple-negative breast cancer; HR, hazard ration; KEGG, Kyoto Encyclopedia of Genes and Genomes; TCGA, The Cancer Genome Atlas.

chromatin structure and the inhibition of gene transcription. Considering that HDAC7 was downregulated in TNBC, its direct targets were presumed to be upregulated. Therefore, the highly expressed genes in TNBC were screened based on TCGA database (Fig. 4A). Genes which were upregulated in TNBC, whose |log 2 (fold change)|>1 and P-value <0.05 were selected. Then co-expression analysis was performed and 10 genes were identified to be significantly associated to HDAC7, including C3orf36, NudCD1, LRRCC1, CHAF1B, CDCA2, ESRP1, SCML2, MSH2, GGH and XYLB. Among them, C3orf36 was positively associated with HDAC7, while the rest of the genes were negatively associated with HDAC7 (P<0.05; Fig. 4B).

The expression levels of these 10 genes were detected by METABRIC database. SCML2 was unavailable in the database. C3orf36 showed a discrete expression pattern consistent with that in TCGA and the other eight genes were all upregulated in TNBC vs. non-TNBC tissue (P<0.0001), consistent with the results from TCGA (Fig. 4C). Kaplan-Meier survival curves indicated that high expression of NudCD1 (HR=2.32, 95%CI=1.04-5.16, P=0.035), GGH (HR=2.38, 95%CI=1.08-5.22, P=0.026) in TCGA

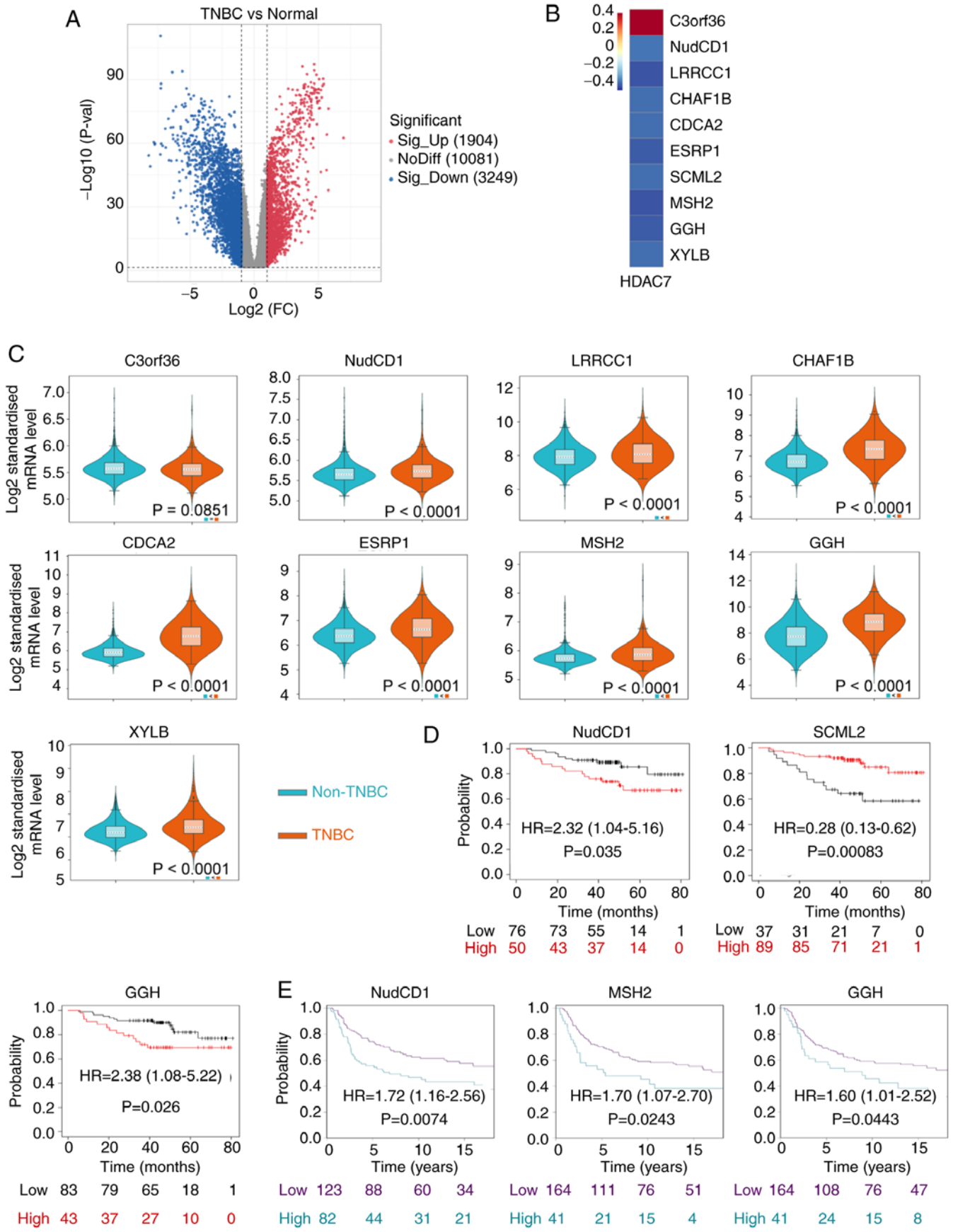

Figure 4. NudCD1 and GGH are prognostic HDAC7-Related downstream genes of HDAC7. (A) Volcano plot of differentially expressed genes between TNBC and normal breast tissue in the TCGA database. (B) Heat map of the negative relation genes with HDAC7, the color represents the P-value. (C) Validation of the correlation genes expression in the METABRIC database, except for C3orf36, all the correlation genes were upregulated in TNBC (P<0.05). (D) Kaplan-Meier survival analysis of correlation genes in the TCGA database. NudCD1, SCML2 and GGH were statistically associated with prognosis in TNBC (P<0.05). (E) Kaplan-Meier survival analysis of correlation genes in the METABRIC database. NudCD1, MSH2 and GGH were statistically associated with prognosis in TNBC (P<0.05). HDACs, histone deacetylases; TNBC, triple-negative breast cancer; TCGA, The Cancer Genome Atlas.

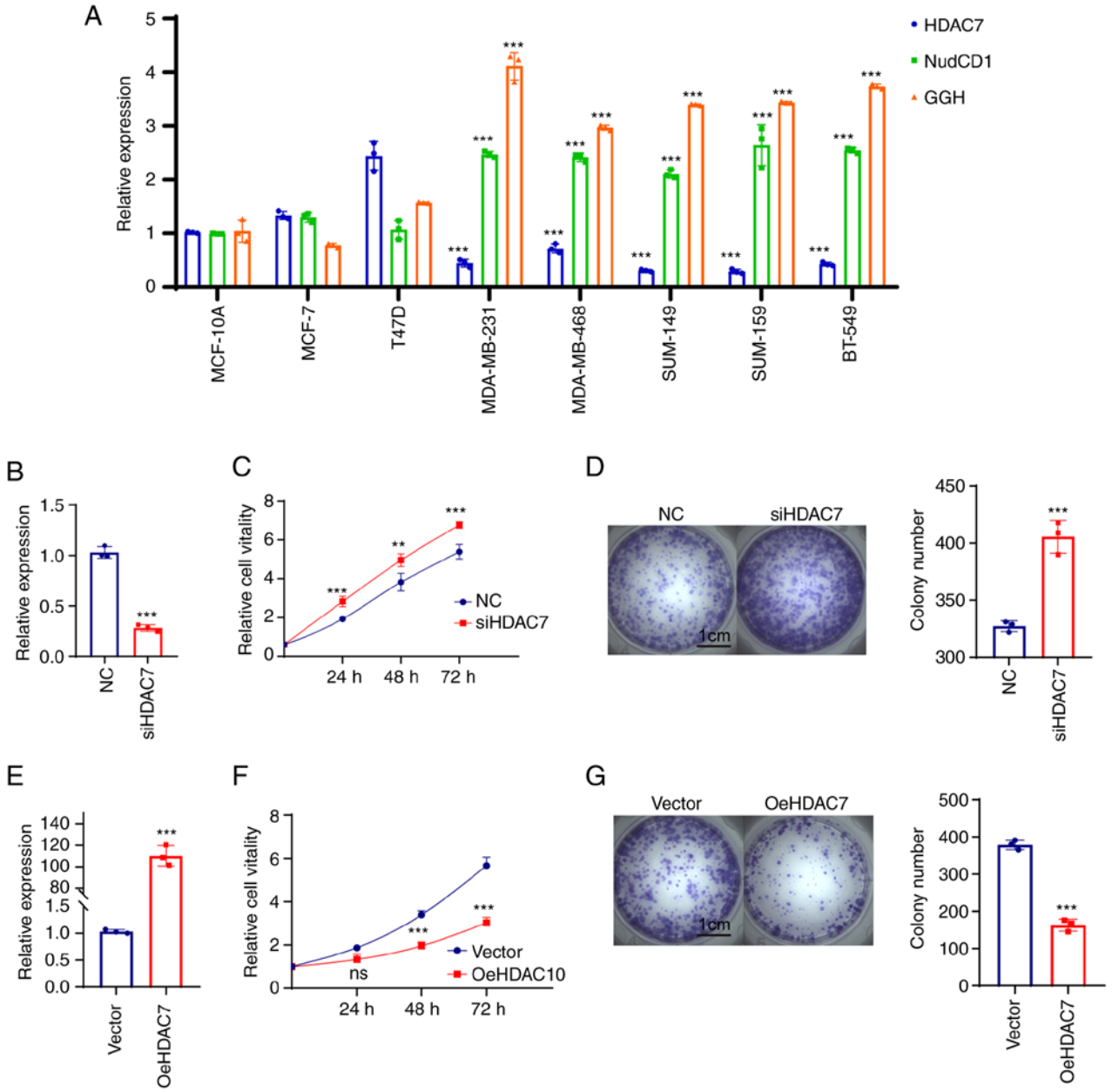

Figure 5. HDAC7 regulated TNBC proliferation *in vitro*. (A) Reverse transcription-quantitative PCR showed the mRNA expression level of HDAC7, NUDCD1 and GGH in the normal breast tissue cell line (MCF-10A), the luminal breast cancer cell lines (MCF-7, T47D) and the TNBC cell lines (MDA-MB-231, MDA-MB-468, SUM-149, SUM-159 and BT-549). (B) Quantitative PCR validation of the siRNA efficiency of HDAC7 in MDA-MB-468 cell line. (C) MTT cell growth curve showed the proliferation capacity after si-HDAC7 in MDA-MB-468 cells. (D) Colony formation assay showed the colony formation capacity after siHDAC7 in MDA-MB-468 cells, statistical graph on the right. (E) Quantitative PCR showed the overexpression efficiency of HDAC7 in SUN-149 cell line. (F) MTT cell growth curve showed the proliferation capacity after oe-HDAC7 in SUM-149 cells. (G) The colony formation assay showed the clone formation ability after oe-HDAC7 in SUM-149 cells, statistical graph on the right. **P<0.01, ***P<0.005. All experiments were repeated three times independently and the results of the statistical graphs were a summary of the three independent results. HDACs, histone deacetylases; TNBC, triple-negative breast cancer; si, small interfering; oe, overexpression; NC, negative control.

database (Fig. 4D) and NudCD1 (HR=1.72, 95%CI=1.16-2.56, P=0.0074), MSH2 (HR=1.70, 95%CI=1.07-2.70, P=0.0243), GGH (HR=1.60, 95%CI=1.01-2.52, P=0.0443) in METABRIC database (Fig. 4E) were significantly associated with poor OS of patients with TNBC. On the other hand, high expression of SCML2 (HR=0.28; 95%CI=0.13-0.62; P=0.00083) was associated with improved OS of patients with TNBC in TCGA database (Fig. 4D). Kaplan-Meier survival analysis for other differentially expressed genes are in Fig. S2 and exhibited no statistical significance.

HDAC7-NudCD1/GGH regulates TNBC cell proliferation in vitro. As NudCD1 and GGH were both prognostic factors in two datasets, the expression and functions of HDAC7-NudCD1/GGH on BRCA cell lines were further verified. RT-qPCR was performed in normal BRCA cell line MCF-10A, luminal BRCA cell lines MCF-7 and T47D and TNBC cell lines MDA-MB-231, MDA-MB-468, MDA-MB-149, MDA-MB-159 and BT-549. The results showed that HDAC7 mRNA level was upregulated in luminal cell lines (MCF-7 and T47D) and significantly downregulated in TNBC cell

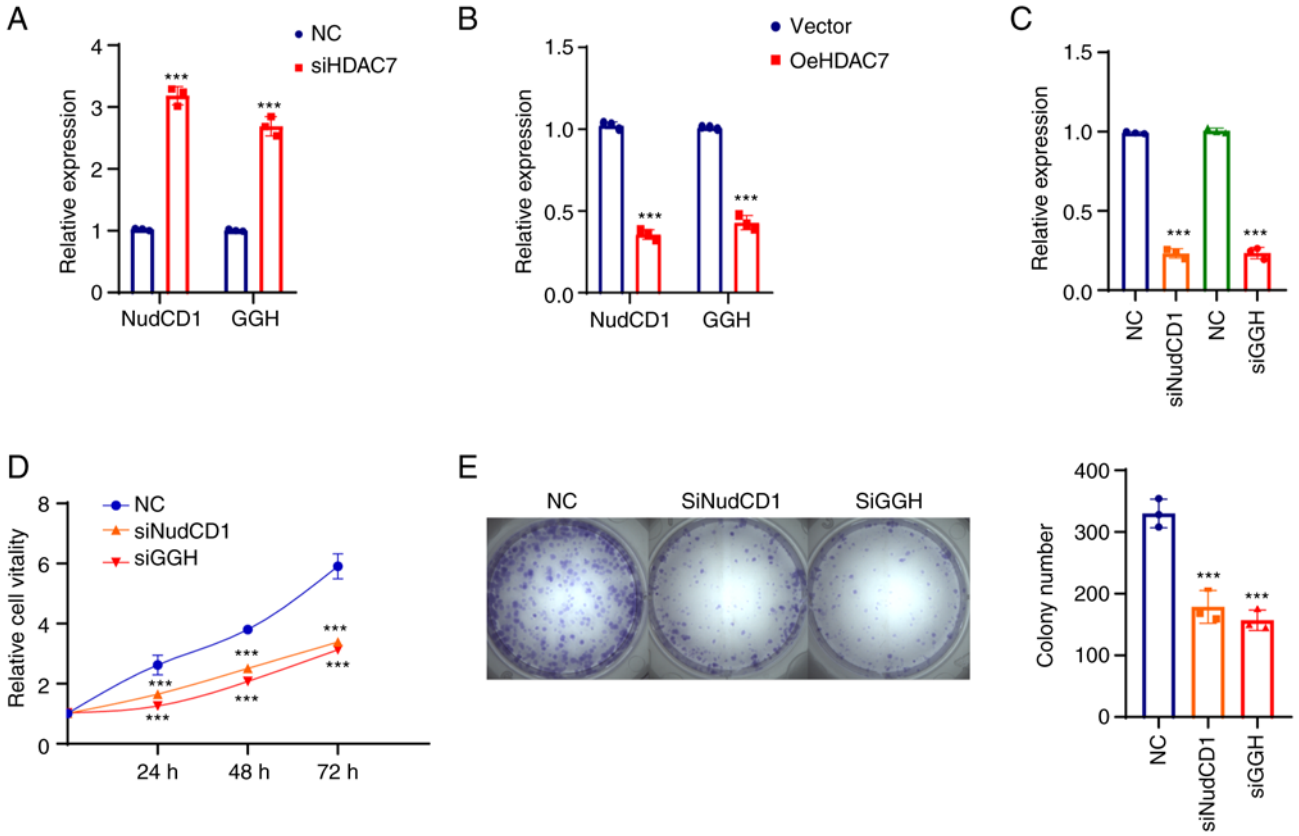

Figure 6. HDAC7-NUDCD1/GGH regulated TNBC proliferation *in vitro*. Quantitative PCR showed after (A) siHDAC7 and (B) oe-HDAC7, the RNA expression of NudCD1 and GGH in (A) MDA-MB-468 cells and (B) SUM-149 cells. (D) Quantitative PCR presented the si-efficiency of NudCD1 and GGH. (D) MTT cell growth curve showed the proliferation capacity after si-NudCD1 and si-GGH in MDA-MB-468 cells. (E) Colony formation assay showed that after knocking down NudCD1 and GGH, colony formation was significantly reduced. Statistical graph on the right. ***P<0.005. All experiments were repeated three times independently and the results of the statistical graphs were a summary of the three independent results. HDACs, histone deacetylases; TNBC, triple-negative breast cancer; si, small interfering; oe, overexpression; NC, negative control.

lines (MDA-MB-231, MDA-MB-468, SUM-149, SUM-159 and BT-549), while NudCD1 and GGH mRNA expression were slightly changed in luminal cell lines but significantly upregulated in TNBC cell lines (Fig. 5A).

Due to the low expression of HDAC7 in TNBC cell lines, cell proliferation was observed in MDA-MB-468 cells which displayed relatively high level of HDAC7 in triple negative breast cancer cell lines following HDAC7 knockdown (Fig. 5B). The results from MTT (Fig. 5C) and colony formation assays (Fig. 5D) showed that silencing of HDAC7 significantly enhanced MDA-MB-468 cell proliferation, suggesting that HDAC7 might play a inhibitory role in TNBC cell growth. The SUM-149 cell line with relatively lower expression of HDAC7 was selected for HDAC7 overexpression experiments. As shown in Fig. 5E, the mRNA level of HDAC7 in the overexpression group was ~100 times higher than that in the negative control group (P<0.05), testifying the overexpression efficiency of HDAC7. As expected, overexpression of HDAC7 inhibited the proliferation of SUN-149 cells (Fig. 5F). Colony formation assay showed that the number of clones in HDAC7 overexpression group was significantly reduced than that in NC group and the size of the colonies was also significantly smaller than that in NC group (Fig. 5G).

Knockdown of HDAC7 increased mRNA expression of NudCD1 and GGH in MDA-MB-468 cells (Fig. 6A) and SUM-149 cells (Fig. 6B), confirming that NudCD1 and GGH were downstream targets of HDAC7. The function of NudCD1 and GGH were further evaluated after NudCD1 and GGH were knocked down in MDA-MB-468 cells and the interference efficacy is shown in Fig. 6C. The proliferation curve showed that knockdown of NudCD1 and GGH inhibited the growth rate (Fig. 6D) and colony formation ability (Fig. 6E) of MDA-MB-468 cells.

Association between prognostic HDAC7-NudCD1/GGH and immune infiltration in TNBC. Immune infiltration has been reported to be associated with TNBC progression and prognosis (42). Since HDAC7, NudCD1 and GGH was screened out to be the prognostic genes for TNBC, the association between immune infiltration and the expression of HDAC7, NudCD1 and GGH was analyzed by the TIMER database (http://timer.cistrome.org/). Then, six immune cell types including CD4+ T cells, CD8+ T cells, NK T cells, γδ T cells, NK cells and macrophages that have been recognized to possess anti-cancer activities were focused on. Immune correlation analysis showed that CD8+ T cell infiltration was negatively associated with HDAC7 (ρ=-0.216), while NK cells (ρ=0.229) and M2 macrophages (ρ=0.248) were positively associated to HDAC7 (P<0.05; Fig. 7A). No significant correlations between M1 macrophages, CD4+ T cells, NK T cells, γδ T cells and HDAC7 (|ρ|<0.2) were observed (Fig. 7B).

CD4+ T cell infiltration was positively associated with GGH (ρ=0.237) and NK cells were negatively associated with

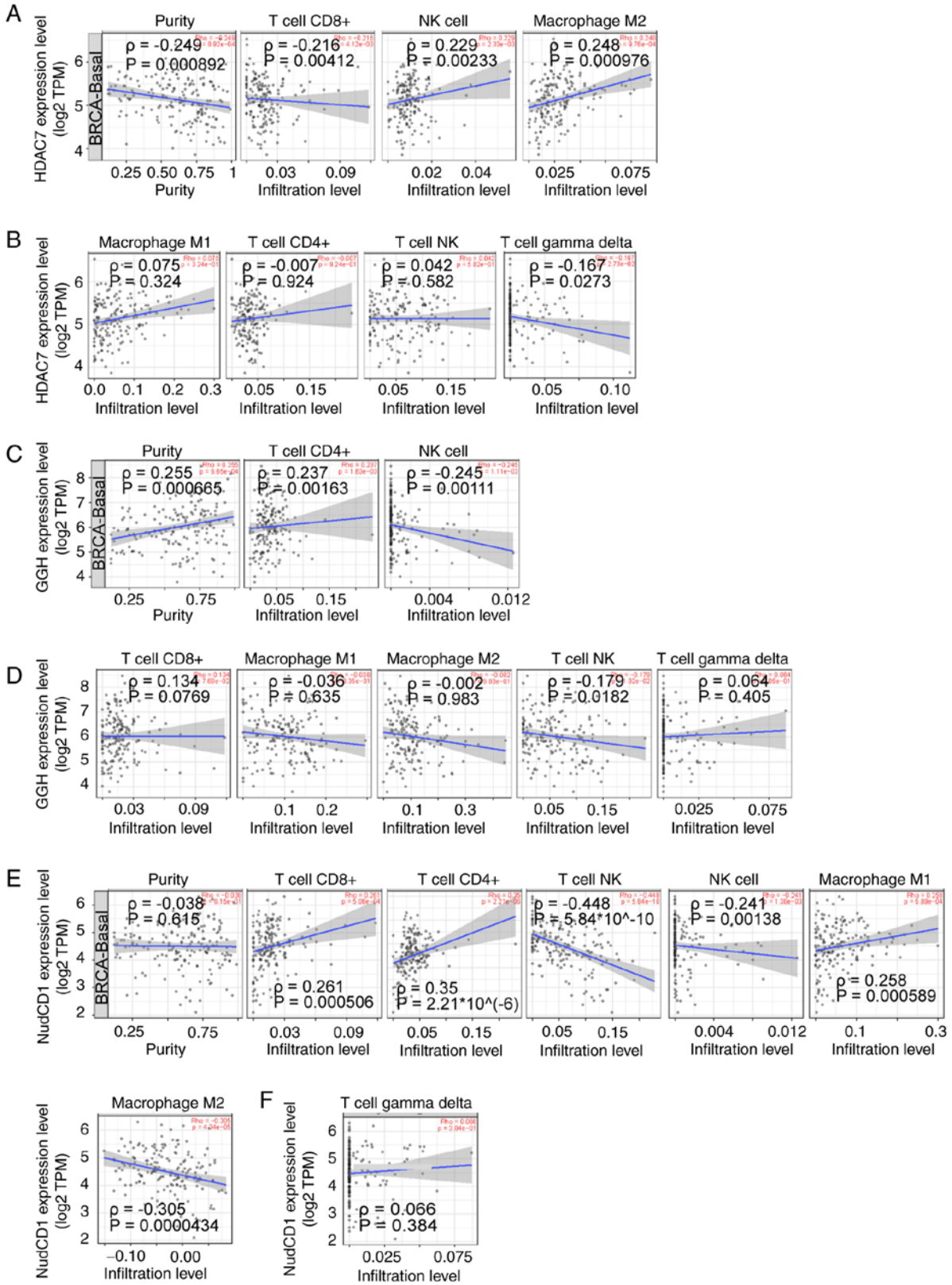

Figure 7. Association between prognostic HDAC7-NudCD1/GGH and immune infiltration in TNBC. (A) Immune cells associated to HDAC7 (P<0.05; |ρ|>0.2). (B) Immune cells without a significant correlation to HDAC7 (|ρ|<0.2). (C) Immune cells associated to GGH (P<0.05; |ρ|>0.2). (D) Immune cells with poor GGH correlation (|ρ|<0.2). (E) Immune cells associated with NudCD1 (P<0.05; |ρ|>0.2). (F) Immune cells with poor NudCD1 correlation (|ρ|<0.2). HDACs, histone deacetylases; TNBC, triple-negative breast cancer.

GGH (ρ=-0.245; P<0.05; Fig. 7C). No significant correlation between M1 macrophages, M2 macrophages, CD8+ T cells, NKT cells, γδ T cells and GGH expression (|R|<0.2) were observed (Fig. 6D). At the same time, CD8+ T cells (ρ=0.261), CD4+ T cells (ρ=0.35) and M1 macrophages (ρ=0.258) were positively associated to NudCD1 (P<0.05). NKT cells

(ρ=-0.448), NK cells (ρ=-0.241) and M2 macrophages (ρ=-0.305) were negatively associated to NudCD1 (P<0.05) (Fig. 7E). No significant correlation between γδ T cells and NudCD1 (|ρ|<0.2) was observed (Fig. 7F). Altogether, these results showed that NK cell infiltration was positively associated with HDAC7 and negatively associated with NudCD1 and GGH expression, suggesting that the anti-tumor effects of HDAC7-NUDCD1/GGH axis might be partially associated with the infiltration of NK cells.

Discussion

The current study was focused on identifying prognostic HDACs in TNBC and investigating possible therapeutic molecules in the downstream. By analyzing the correlation between the expression of HDAC1-11 and overall survival of patients with TNBC via the TCGA and METABRIC databases, HDAC7, a class II HDAC, was discovered to be significantly downregulated in TNBC samples and positively associated with OS of patients with TNBC. These results indicated that HDAC7 might be a tumor suppressor in TNBC. However, previous studies have revealed controversial functions of HDAC7 in cancer progression. HDAC7 has been previously reported to promote tumor progression in lung cancer via inhibiting STAT3 activation and upregulating FGF18 (43,44). HDAC7 has been reported to be regulated by ZNF326, activates Wnt pathway and promotes malignant phenotypes of glioblastoma (45). At the same time, HDAC7 has been revealed to deacetylate AGO2 and inhibit the biogenesis of miR-19b human alveolar adenocarcinoma basal epithelial cells and cervical cancer cells, hence inhibiting cancer development (46). A previous study showed that absence of HDAC7 can induce TET2 expression, promote DNA 5-hydroxymethelation and chromatin de-condensation in B cell lymphocytes, hence leading to B cell-based hematological malignancies (47). In pro-B acute lymphoblastic leukemia and Burkitt lymphoma, HDAC7 has been shown to be unexpressed and the re-expression of HDAC7 in animal models has a potent anti-tumor effect (48). HDAC7 has been reported to epigenetically inhibit the angiogenesis suppressor gene AKAP12 and reduce the formation of tube-like structures (49). It has been also documented that HDAC7 can maintain cancer stem cells and contribute to tumor progression in BRCA and ovarian tumors (50-52). All these findings indicate the comprehensive and complex effects of HDAC7 in cancers. In TNBC, Uzelac *et al* (53) found that HDAC7 expression is lower in TNBC samples compared with samples of ER+/PR+/HER2-tumors and the high expression of HDAC7 represented poor survival in patients with TNBC (HR=9.287; P=0.033). This finding is different from the results of the present study, possibly due to the difference in the number of patients and the heterogeneity between patients. In the present study, a total of 123 patients with TNBC and 363 patients with TNBC were respectively covered in TCGA and METABIRC database, while the number of patients with TNBC in Uzelac *et al* (53) is only 61. For further validation, a larger number of cases are required. Therefore, the role of HDAC7 in TNBC has yet to be fully elucidated. In further analysis of the TCGA database, it was found that HDAC7 was associated with proliferation-related pathways including the PI3K-AKT pathway and the Ras signaling pathway. Meanwhile, the cytokine-cytokine linkage pathway was also associated with HDAC7, indicating that HDAC7 might regulate the progression of TNBC by mediating these growth and immune-related pathways, which needed further experimental validation.

A novel finding of the present study was that NudCD1 and GGH were identified as the target genes of HDAC7. NudCD1 and GGH were negatively regulated by HDAC7 and associated with poor prognosis in TNBC. NudCD1 has been shown to drive the proliferation, migration and invasion of lung cancer and colorectal cancer cells (54,55). GGH has also been reported to be associated with poor prognosis and unfavorable clinical outcomes in invasive patients with BRCA (56). Elevated GGH expression is associated with poor prognosis in uterine corpus endometrial carcinoma and advanced gastric cancer (57,58). Nonetheless, the roles of NudCD1 and GGH in TNBC remain elusive. The present study found that silencing of HDAC7 upregulated NudCD1 and GGH expression in TNBC cell lines, indicating that NudCD1 and GGH might be negatively regulated by HDAC7. Furthermore, knockdown of HDAC7 potentiated the proliferation while knockdown of NudCD1 or GGH inhibited the proliferation of TNBC cells *in vitro*. The present study showed that decrease of HDAC7 might promote the proliferation of TNBC cells by activating NudCD1/GGH axis and indicated that inhibition of NudCD1/GGH might axis be a possible therapeutic therapy for TNBC.

The immune microenvironment is widely considered to have a vital role in the tumor progression. TNBC is reported to be an immune 'hot' subtype of BRCA with high immune cell infiltration, for which immunotherapy may be a viable treatment strategy (59). Hence, the immune regulatory roles of HDAC7-NudCD1/GGH axis was explored via analyzing the correlation between prognostic factors and immune infiltration. NK cells are one of the main effector immune cells that play an anti-cancer role. Studies have supported that low infiltration of NK cells in tumor tissues is associated with poor outcome (60,61). However, therapy based on infused NK cells has been mainly applied to hematologic malignancies, so far with limited therapeutic effect in patients with solid tumor patients (62,63). The present study showed that HDAC7-NudCD1/GGH axis was associated with the density of NK cells, which indicated that HDAC7 might exert its anti-tumor roles partially by regulating NK cell infiltration through blocking the NudCD1/GGH axis. Nevertheless, this finding still needs further validation. In brief, the present study revealed a novel role of the HDAC7-NudCD1/GGH axis in TNBC.

Acknowledgements

Not applicable.

Funding

The present study was funded by Natural Science Foundation of Guangdong Province (grant no. 2022A1515012166) and Natural Science Foundation of China (grant no. 82003176).

Availability of data and materials

The datasets used and/or analyzed during the current study are available from the corresponding author on reasonable request.

Authors' contributions

YL, HL and MZ conceived the idea and designed the present study. NL collected the data from databases and performed analyses. MZ, JL and JW conducted the *in vitro* experiments. MZ organized and arranged all the figures. MZ. and YL wrote the manuscript. All authors read and approved the final manuscript. MZ and NL confirm the authenticity of all the raw data.

Ethics approval and consent to participate

Not applicable.

Patient consent for publication

Not applicable.

Competing interests

The authors declare that they have no competing interests.

References

1. Sung H, Ferlay J, Siegel RL, Laversanne M, Soerjomataram I, Jemal A and Bray F: Global cancer statistics 2020: GLOBOCAN estimates of incidence and mortality worldwide for 36 cancers in 185 countries. CA Cancer J Clin 71: 209-249, 2021.
2. Loibl S, Poortmans P, Morrow M, Denkert C and Curigliano G: Breast cancer. Lancet 397: 1750-1769, 2021.
3. Barzaman K, Karami J, Zarei Z, Hosseinzadeh A, Kazemi MH, Moradi-Kalbolandi S, Safari E and Farahmand L: Breast cancer: Biology, biomarkers, and treatments. Int Immunopharmacol 84: 106535, 2020.
4. Won KA and Spruck C: Triple-negative breast cancer therapy: Current and future perspectives (Review). Int J Oncol 57: 1245-1261, 2020.
5. Waks AG and Winer EP: Breast cancer treatment: A review. JAMA 321: 288-300, 2019.
6. Portela A and Esteller M: Epigenetic modifications and human disease. Nat Biotechnol 28: 1057-1068, 2010.
7. Lu Y, Chan YT, Tan HY, Li S, Wang N and Feng Y: Epigenetic regulation in human cancer: The potential role of epi-drug in cancer therapy. Mol Cancer 19: 79, 2020.
8. Garcia-Martinez L, Zhang Y, Nakata Y, Chan HL and Morey L: Epigenetic mechanisms in breast cancer therapy and resistance. Nat Commun 12: 1786, 2021.
9. Shvedunova M and Akhtar A: Modulation of cellular processes by histone and non-histone protein acetylation. Nat Rev Mol Cell Biol 23: 329-349, 2022.
10. Sun L, Zhang H and Gao P: Metabolic reprogramming and epigenetic modifications on the path to cancer. Protein Cell 13: 877-919, 2022.
11. Witt O, Deubzer HE, Milde T and Oehme I: HDAC family: What are the cancer relevant targets? Cancer Lett 277: 8-21, 2009.
12. Falkenberg KJ and Johnstone RW: Histone deacetylases and their inhibitors in cancer, neurological diseases and immune disorders. Nat Rev Drug Discov 13: 673-691, 2014.
13. Ho TCS, Chan AHY and Ganesan A: Thirty years of HDAC inhibitors: 2020 Insight and hindsight. J Med Chem 63: 12460-12484, 2020.
14. Hesham HM, Lasheen DS and Abouzid KAM: Chimeric HDAC inhibitors: Comprehensive review on the HDAC-based strategies developed to combat cancer. Med Res Rev 38: 2058-2109, 2018.
15. Brancolini C, Gagliano T and Minisini M: HDACs and the epigenetic plasticity of cancer cells: Target the complexity. Pharmacol Ther 238: 108190, 2022.
16. Ediriweera MK, Tennekoon KH and Samarakoon SR: Emerging role of histone deacetylase inhibitors as anti-breast-cancer agents. Drug Discov Today 24: 685-702, 2019.
17. Dowling CM, Hollinshead KER, Di Grande A, Pritchard J, Zhang H, Dillon ET, Haley K, Papadopoulos E, Mehta AK, Bleach R, *et al*: Multiple screening approaches reveal HDAC6 as a novel regulator of glycolytic metabolism in triple-negative breast cancer. Sci Adv 7: eabc4897, 2021.
18. Oba T, Ono M, Matoba H, Uehara T, Hasegawa Y and Ito KI: HDAC6 inhibition enhances the anti-tumor effect of eribulin through tubulin acetylation in triple-negative breast cancer cells. Breast Cancer Res Treat 186: 37-51, 2021.
19. Wang ZT, Chen ZJ, Jiang GM, Wu YM, Liu T, Yi YM, Zeng J, Du J and Wang HS: Histone deacetylase inhibitors suppress mutant p53 transcription via HDAC8/YY1 signals in triple negative breast cancer cells. Cell Signal 28: 506-515, 2016.
20. Wu S, Luo Z, Yu PJ, Xie H and He YW: Suberoylanilide hydroxamic acid (SAHA) promotes the epithelial mesenchymal transition of triple negative breast cancer cells via HDAC8/FOXA1 signals. Biol Chem 397: 75-83, 2016.
21. Palmieri D, Lockman PR, Thomas FC, Hua E, Herring J, Hargrave E, Johnson M, Flores N, Qian Y, Vega-Valle E, *et al*: Vorinostat inhibits brain metastatic colonization in a model of triple-negative breast cancer and induces DNA double-strand breaks. Clin Cancer Res 15: 6148-6157, 2009.
22. Tate CR, Rhodes LV, Segar HC, Driver JL, Pounder FN, Burow ME and Collins-Burow BM: Targeting triple-negative breast cancer cells with the histone deacetylase inhibitor panobinostat. Breast Cancer Res 14: R79, 2012.
23. Rhodes LV, Tate CR, Segar HC, Burks HE, Phamduy TB, Hoang V, Elliott S, Gilliam D, Pounder FN, Anbalagan M, *et al*: Suppression of triple-negative breast cancer metastasis by pan-DAC inhibitor panobinostat via inhibition of ZEB family of EMT master regulators. Breast Cancer Res Treat 145: 593-604, 2014.
24. Zhang K, Liu Z, Yao Y, Qiu Y, Li F, Chen D, Hamilton DJ, Li Z and Jiang S: Structure-based design of a selective class I histone deacetylase (HDAC) near-infrared (NIR) probe for epigenetic regulation detection in triple-negative breast cancer (TNBC). J Med Chem 64: 4020-4033, 2021.
25. Pinkerneil M, Hoffmann MJ, Deenen R, Köhrer K, Arent T, Schulz WA and Niegisch G: Inhibition of class I histone deacetylases 1 and 2 promotes urothelial carcinoma cell death by various mechanisms. Mol Cancer Ther 15: 299-312, 2016.
26. Sulaiman A, McGarry S, Lam KM, El-Sahli S, Chambers J, Kaczmarek S, Li L, Addison C, Dimitroulakos J, Arnaout A, *et al*: Co-inhibition of mTORC1, HDAC and ESR1α retards the growth of triple-negative breast cancer and suppresses cancer stem cells. Cell Death Dis 9: 815, 2018.
27. Ma W, Sun J, Xu J, Luo Z, Diao D, Zhang Z, Oberly PJ, Minnigh MB, Xie W, Poloyac SM, *et al*: Sensitizing triple negative breast cancer to tamoxifen chemotherapy via a redox-responsive vorinostat-containing polymeric prodrug nanocarrier. Theranostics 10: 2463-2478, 2020.
28. Torres-Adorno AM, Lee J, Kogawa T, Ordentlich P, Tripathy D, Lim B and Ueno NT: Histone deacetylase inhibitor enhances the efficacy of MEK inhibitor through NOXA-mediated MCL1 degradation in triple-negative and inflammatory breast cancer. Clin Cancer Res 23: 4780-4792, 2017.
29. Min A, Im SA, Kim DK, Song SH, Kim HJ, Lee KH, Kim TY, Han SW, Oh DY, Kim TY, *et al*: Histone deacetylase inhibitor, suberoylanilide hydroxamic acid (SAHA), enhances anti-tumor effects of the poly (ADP-ribose) polymerase (PARP) inhibitor olaparib in triple-negative breast cancer cells. Breast Cancer Res 17: 33, 2015.
30. Huang JP and Ling K: EZH2 and histone deacetylase inhibitors induce apoptosis in triple negative breast cancer cells by differentially increasing H3 Lys^{27} acetylation in the BIM gene promoter and enhancers. Oncol Lett 14: 5735-5742, 2017.
31. Wiegmans AP, Yap PY, Ward A, Lim YC and Khanna KK: Differences in expression of key DNA damage repair genes after epigenetic-induced brcaness dictate synthetic lethality with PARP1 inhibition. Mol Cancer Ther 14: 2321-2331, 2015.
32. Rao R, Balusu R, Fiskus W, Mudunuru U, Venkannagari S, Chauhan L, Smith JE, Hembruff SL, Ha K, Atadja P and Bhalla KN: Combination of pan-histone deacetylase inhibitor and autophagy inhibitor exerts superior efficacy against triple-negative human breast cancer cells. Mol Cancer Ther 11: 973-983, 2012.
33. Garmpis N, Damaskos C, Garmpi A, Kalampokas E, Kalampokas T, Spartalis E, Daskalopoulou A, Valsami S, Kontos M, Nonni A, *et al*: Histone deacetylases as new therapeutic targets in triple-negative breast cancer: Progress and promises. Cancer Genomics Proteomics 14: 299-313, 2017.
34. Jiang Z, Li W, Hu X, Zhang Q, Sun T, Cui S, Wang S, Ouyang Q, Yin Y, Geng C, *et al*: Tucidinostat plus exemestane for postmenopausal patients with advanced, hormone receptor-positive breast cancer (ACE): A randomised, double-blind, placebo-controlled, phase 3 trial. Lancet Oncol 20: 806-815, 2019.

35. Chiu HW, Yeh YL, Wang YC, Huang WJ, Ho SY, Lin P and Wang YJ: Combination of the novel histone deacetylase inhibitor YCW1 and radiation induces autophagic cell death through the downregulation of BNIP3 in triple-negative breast cancer cells in vitro and in an orthotopic mouse model. Mol Cancer 15: 46, 2016.
36. da Silva JL, Cardoso Nunes NC, Izetti P, de Mesquita GG and de Melo AC: Triple negative breast cancer: A thorough review of biomarkers. Crit Rev Oncol Hematol 145: 102855, 2020.
37. Ritchie ME, Phipson B, Wu D, Hu Y, Law CW, Shi W and Smyth GK: limma powers differential expression analyses for RNA-sequencing and microarray studies. Nucleic Acids Res 43: e47, 2015.
38. R Core Team. R: A language and environment for statistical computing. R Foundation for Statistical Computing, Vienna, Austria, 2022. URL http://www.R-project.org/.
39. Kuemmerlen D, Echtermann T, Muentener C and Sidler X: Agreement of benchmarking high antimicrobial usage farms based on either animal treatment index or number of national defined daily doses. Front Vet Sci 7: 638, 2020.
40. Li T, Fu J, Zeng Z, Cohen D, Li J, Chen Q, Li B and Liu XS: TIMER2.0 for analysis of tumor-infiltrating immune cells. Nucleic Acids Res 48 (W1): W509-W514, 2020.
41. Nolan T, Hands RE and Bustin SA: Quantification of mRNA using real-time RT-PCR. Nat Protoc 1: 1559-1582, 2006.
42. Keenan TE and Tolaney SM: Role of immunotherapy in triple-negative breast cancer. J Natl Compr Canc Netw 18: 479-489, 2020.
43. Guo K, Ma Z, Zhang Y, Han L, Shao C, Feng Y, Gao F, Di S, Zhang Z, Zhang J, *et al*: HDAC7 promotes NSCLC proliferation and metastasis via stabilization by deubiquitinase USP10 and activation of β-catenin-FGF18 pathway. J Exp Clin Cancer Res 41: 91, 2022.
44. Lei Y, Liu L, Zhang S, Guo S, Li X, Wang J, Su B, Fang Y, Chen X, Ke H and Tao W: Hdac7 promotes lung tumorigenesis by inhibiting Stat3 activation. Mol Cancer 16: 170, 2017.
45. Yu X, Wang M, Wu J, Han Q and Zhang X: ZNF326 promotes malignant phenotype of glioma by up-regulating HDAC7 expression and activating Wnt pathway. J Exp Clin Cancer Res 38: 40, 2019.
46. Zhang H, Wang Y, Dou J, Guo Y, He J, Li L, Liu X, Chen R, Deng R, Huang J, *et al*: Acetylation of AGO2 promotes cancer progression by increasing oncogenic miR-19b biogenesis. Oncogene 38: 1410-1431, 2019.
47. Azagra A, Meler A, de Barrios O, Tomás-Daza L, Collazo O, Monterde B, Obiols M, Rovirosa L, Vila-Casadesús M, Cabrera-Pasadas M, *et al*: The HDAC7-TET2 epigenetic axis is essential during early B lymphocyte development. Nucleic Acids Res 50: 8471-8490, 2022.
48. Barneda-Zahonero B, Collazo O, Azagra A, Fernández-Duran I, Serra-Musach J, Islam AB, Vega-Garcia N, Malatesta R, Camós M, Gómez A, *et al*: The transcriptional repressor HDAC7 promotes apoptosis and c-Myc downregulation in particular types of leukemia and lymphoma. Cell Death Dis 6: e1635, 2015.
49. Turtoi A, Mottet D, Matheus N, Dumont B, Peixoto P, Hennequiere V, Deroanne C, Colige A, De Pauw E, Bellahcène A and Castronovo V: The angiogenesis suppressor gene AKAP12 is under the epigenetic control of HDAC7 in endothelial cells. Angiogenesis 15: 543-554, 2012.
50. Caslini C, Hong S, Ban YJ, Chen XS and Ince TA: HDAC7 regulates histone 3 lysine 27 acetylation and transcriptional activity at super-enhancer-associated genes in breast cancer stem cells. Oncogene 38: 6599-6614, 2019.
51. Cutano V, Di Giorgio E, Minisini M, Picco R, Dalla E and Brancolini C: HDAC7-mediated control of tumour microenvironment maintains proliferative and stemness competence of human mammary epithelial cells. Mol Oncol 13: 1651-1668, 2019.
52. Witt AE, Lee CW, Lee TI, Azzam DJ, Wang B, Caslini C, Petrocca F, Grosso J, Jones M, Cohick EB, *et al*: Identification of a cancer stem cell-specific function for the histone deacetylases, HDAC1 and HDAC7, in breast and ovarian cancer. Oncogene 36: 1707-1720, 2017.
53. Uzelac B, Krivokuca A, Susnjar S, Milovanovic Z and Supic G: Histone deacetylase 7 gene overexpression is associated with poor prognosis of triple-negative breast cancer patients. Genet Test Mol Biomarkers 25: 227-235, 2021.
54. Han B, Zhang YY, Xu K, Bai Y, Wan LH, Miao SK, Zhang KX, Zhang HW, Liu Y and Zhou LM: NUDCD1 promotes metastasis through inducing EMT and inhibiting apoptosis in colorectal cancer. Am J Cancer Res 8: 810-823, 2018.
55. He B, Xia S and Zhang Z: NudCD1 promotes the proliferation and metastasis of non-small cell lung cancer cells through the activation of IGF1R-ERK1/2. Pathobiology 87: 244-253, 2020.
56. Shubbar E, Helou K, Kovács A, Nemes S, Hajizadeh S, Enerbäck C and Einbeigi Z: High levels of γ-glutamyl hydrolase (GGH) are associated with poor prognosis and unfavorable clinical outcomes in invasive breast cancer. BMC Cancer 13: 47, 2013.
57. Yu C, Qi H, Zhang Y, Zhao W and Wu G: Elevated expression of gamma-glutamyl hydrolase is associated with poor prognosis and altered immune signature in uterine corpus endometrial carcinoma. Front Genet 12: 764194, 2022.
58. Maezawa Y, Sakamaki K, Oue N, Kimura Y, Hashimoto I, Hara K, Kano K, Aoyama T, Hiroshima Y, Yamada T, *et al*: High gamma-glutamyl hydrolase and low folylpolyglutamate synthetase expression as prognostic biomarkers in patients with locally advanced gastric cancer who were administrated postoperative adjuvant chemotherapy with S-1. J Cancer Res Clin Oncol 146: 75-86, 2020.
59. Avella Patino DM, Radhakrishnan V, Suvilesh KN, Manjunath Y, Li G, Kimchi ET, Staveley-O'Carroll KF, Warren WC, Kaifi JT and Mitchem JB: Epigenetic regulation of cancer immune cells. Semin Cancer Biol 83: 377-383, 2022.
60. Albertsson PA, Basse PH, Hokland M, Goldfarb RH, Nagelkerke JF, Nannmark U and Kuppen PJ: NK cells and the tumour microenvironment: Implications for NK-cell function and anti-tumour activity. Trends Immunol 24: 603-609, 2003.
61. Wu SY, Fu T, Jiang YZ and Shao ZM: Natural killer cells in cancer biology and therapy. Mol Cancer 19: 120, 2020.
62. Lorenzo-Herrero S, López-Soto A, Sordo-Bahamonde C, Gonzalez-Rodriguez AP, Vitale M and Gonzalez S: NK cell-based immunotherapy in cancer metastasis. Cancers (Basel) 11: 29, 2018.
63. Bald T, Krummel MF, Smyth MJ and Barry KC: The NK cell-cancer cycle: Advances and new challenges in NK cell-based immunotherapies. Nat Immunol 21: 835-847, 2020.